

Answer to the comments on Confirming geomagnetic Sfe by means of a solar flare detector based on GNSS

Juan José Curto^{1*}, Jose Miguel Juan², Cristhian Camilo Timoté²

¹ Observatorio del Ebro, (OE) CSIC – Universitat Ramon Llull (URL), 43520 Roquetes, Spain

² Research group on Astronomy and Geomatics (gAGE), Universitat Politècnica de Catalunya (UPC) Jordi Girona 1–3, 08034 Barcelona, Spain

e-mail: jjcurto@obsebre.es, jose.miguel.juan@upc.edu, cristhian.timote@upc.edu

ABSTRACT

Hernández-Pajares and García-Rigo have written a document criticizing our paper “*Confirming geomagnetic Sfe by means of a solar flare detector based on GNSS*”, *J. Space Weather Space Clim.* 10 9, A42, <https://doi.org/10.1051/swsc/2019040> (Curto et al., 2019). The main goal of our paper was to define a methodology based on GNSS measurements that is able to detect solar flares (SF) in an automatic way. This methodology was used to confirm Sfe (SF effects) detected by geomagnetism in an unsupervised manner. In their document, Hernández-Pajares and García-Rigo posed two objections related to the correctness and the novelty of the methodology used in our paper. This document is a reply to these objections and concludes that they are not relevant.

1. Introduction

The aim of the work presented in Curto et al., (2019) was to define a methodology based on GNSS measurements that is able to detect solar flares (SF) in an automatic way, to confirm solar flare effects (Sfe) detected by geomagnetism in an unsupervised manner.

The basic measurements used to define the SF detector presented in Curto et al., (2019) are the slant total electron content (STEC) variations, corrected by an obliquity factor (see below). This obliquity factor was introduced to reduce the increase in STEC variations at low elevations, i.e. to normalise such STEC variations.

Based on these corrected STEC values, denoted as $\Delta STEC_i^j$, we analysed three candidates for this automatic detector during an entire solar cycle (see Curto et al., (2019) for more information):

1. $\Delta STEC$ at the subsolar point (SSP).
2. $\Delta^2 STEC$ at the subsolar point (SSP).
3. Correlation coefficient, ρ , of the $\Delta^2 STEC$ fitting.

Our work concluded that the combined use of the $\Delta^2 STEC$ and ρ detectors provides a successful ratio of Sfe confirmations.

The comments received by Hernández-Pajares and García-Rigo (hereafter HP&GR) regarding our paper can be summarized as follows:

- 1.- Mistakes in the methodology could invalidate our results.
- 2.- The SF detectors used in our paper were already defined in their papers.

The present document aims to refute these objections.

2. Regarding the claim about mistakes in the methodology.

It is clear that HP&GR assume a single-layer model for the ionosphere, where the obliquity factor is a factor that converts the vertical total electron content (VTEC) to the slant total electron content (STEC) in such a way that, for a satellite “j” and a receiver “i”, the ionospheric delay can be written as:

$$STEC_i^j = m(\varepsilon) \cdot VTEC(A) \quad (1)$$

Where A is the ionospheric pierce point (IPP) (i.e. the intersection of the line of sight vector with the ionospheric layer) and $m(\varepsilon)$ is the so-called obliquity factor or mapping function, defined as:

$$m(\varepsilon) = \sqrt{\frac{1}{1 - \left(\frac{R_E \cdot \cos(\varepsilon)}{R_E + h_{ion}}\right)^2}}$$

Where R_E is the Earth radius, ε is the satellite elevation angle, and h_{ion} is the height of the ionospheric layer.

In GNSS, one of the basic ionospheric measurements for extracting STEC in (1) is the well-known geometry-free combination of carrier-phase (L_{GF}), that shall be corrected from geometric effects such as antenna phase centres (of both satellite and receiver) and from the satellite wind-up. L_{GF} is related to the STEC by:

$$L_{GF_i}^j = STEC_i^j + B_{GF_i}^j$$

Where $B_{GF_i}^j$ is a constant per arc, which includes the so-called carrier phase ambiguities and instrumental biases (of both the satellite and the receiver).

If $B_{IF_i}^j$ is known, thence VTEC can be obtained from the L_{GF} measurements through:

$$VTEC(A) = \frac{1}{m(\varepsilon)} (L_{GF_i}^j - B_{GF_i}^j)$$

Therefore, using the previous relationship one could relate an increase of VTEC at A with the occurrence of a SF.

However, the knowledge of $B_{IF_i}^j$ is not trivial. Therefore, it is common to cancel this term by taking differences on time of $L_{GF_i}^j$ along a continuous arc of data, where it is assumed that $B_{IF_i}^j$ is constant. Thus, this differences on time can be identified with differences of $STEC_i^j$:

$$L_{GF_i}^j(t_B) - L_{GF_i}^j(t_A) = STEC_i^j(t_B) - STEC_i^j(t_A)$$

Where A and B are the IPPs at the times t_A and t_B , respectively.

Applying (1), the previous relationship can be written as:

$$L_{GF_i}^j(t_B) - L_{GF_i}^j(t_A) = m(\varepsilon_B) \cdot VTEC(B) - m(\varepsilon_A) \cdot VTEC(A)$$

Following the HP&GR reasoning this last expression could be approximated as:

$$L_{GF_i}^j(t_B) - L_{GF_i}^j(t_A) \approx m(\varepsilon_A) \cdot \Delta VTEC(A)$$

Therefore, the increase of VTEC at the IPP can be approximated by:

87
$$\Delta VTEC(A) \approx \frac{1}{m(\varepsilon_A)} \left(L_{GF_i}^j(t_B) - L_{GF_i}^j(t_A) \right) \quad (2)$$

88

89 This is the expression that HP&GR are thinking on their first comment.

90

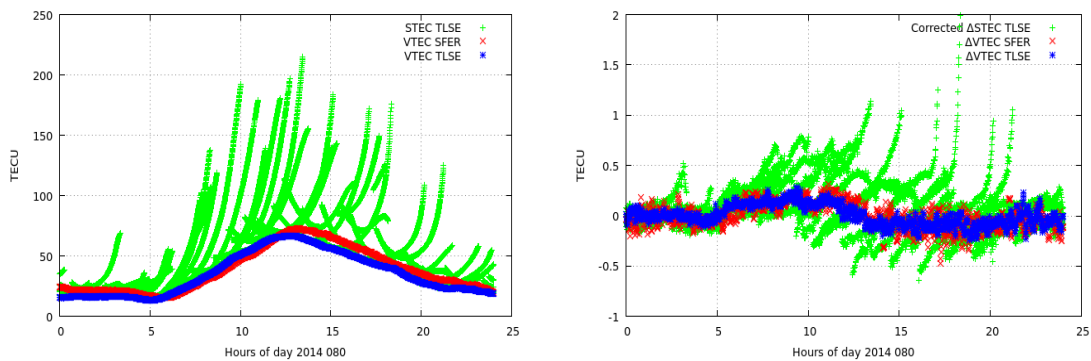
91 However, interpreting the right side of equation (2) as a VTEC variation is just an approximation
 92 that assumes that the STEC variations are linked to an increase of the VTEC at the IPP A. This
 93 assumption would be only true for a geostationary satellite, where both, A and B, are the same
 94 IPP. Nevertheless, in general, STEC variations depends also on the spatial gradients which, at low
 95 elevations, use to be, by far, the predominant component of the STEC variations.

96

97 In order to illustrate the dependency of the STEC variations on the spatial gradient, next Figure
 98 1 depicts, in the left panel, the STEC values for the receiver TLSE (South of France) during the
 99 day 080 in 2014. These STEC values, in green, are obtained after solving, for each arc, the
 100 constant $B_{GF_i}^j$. The solution for these constants are computed by means of a sophisticated
 101 process that includes worldwide carrier phase ambiguity fixing (see Rovira-Garcia et al. (2016)
 102 for more details). Beside these very accurate STEC values, the VTEC values for TLSE and SFER
 103 (South of Spain) are also depicted in the left panel. The VTEC values are obtained from these
 104 very accurate STECs and using a dual layer ionospheric model that, as it is shown in Rovira-Garcia
 105 et al. (2016) or in Rovira-Garcia et al. (2019), is several times more accurate than the standard
 106 single layer ionospheric models. In the right panel, the difference of these three magnitudes
 107 along 1 minute are depicted. As it can be seen, while the VTEC variations (computed from the
 108 ionospheric model) are less than 0.2 TECU (1 TECU=10¹⁶ electrons/m²), the STEC variations
 109 (computed directly using equation (2)) can be larger than 1 TECU (even if one puts and elevation
 110 mask of 20 degrees). These larger variations of the STECs cannot be attributed to the possible
 111 low latitude of the IPPs (this is the reason we depict also the VTEC for SFER). Thus, the variations
 112 in the right side of equation (2) are far from being a VTEC variation.

113

114



115 **Figure 1:** Left panel, STEC values from the receiver TLSE (green), VTEC at TLSE (blue) and VTEC
 116 at SFER (red). Right panel, corrected variations of the STECs in the left panel (green) and
 117 variations of VTEC (blue and red).

118

119 Therefore, in our paper, we interpreted the right side of equation (2) as it is: a STEC variation
 120 multiplied by an obliquity factor ($M(\varepsilon_A) = \frac{1}{m(\varepsilon_A)}$) which mitigates the large variations of STEC at
 121 low elevations. Thus, we define $\Delta STEC_i^j$ as this corrected (normalised) STEC variation:

122
$$\Delta STEC_i^j = M(\varepsilon_A) \cdot \left(L_{GF_i}^j(t_B) - L_{GF_i}^j(t_A) \right) \quad (3)$$

123 This is the definition done in Curto et al., (2019).

124

125 In our opinion this is a more general interpretation than considering this as a VTEC variation at
126 a specific IPP. This different interpretation (in fact, just a different name) for the same
127 measurement is the origin of the two supposed mistakes that HP&GR claim in their comments:

128

129 *First mistake:* “The difference of ionospheric carrier phases in the same phase-continuous
130 transmitter-receiver arc, provides directly the STEC variation, without the need of any mapping
131 function term”

132

133 *Answer:* In our paper, we clearly defined $\Delta STEC_i^j$ as the STEC variations corrected by the
134 obliquity factor. As we have explained, considering $\Delta STEC_i^j$ as a VTEC variation at a given IPP is
135 just a rough approach.

136

137 Second mistake: “In GSFLAI the linear dependence is in terms of the Vertical TEC variation, not
138 the Slant TEC one”.

139

140 *Answer:* This could have happened if we had defined $\Delta STEC_i^j$ without correcting from the
141 obliquity factor, but this not the case.

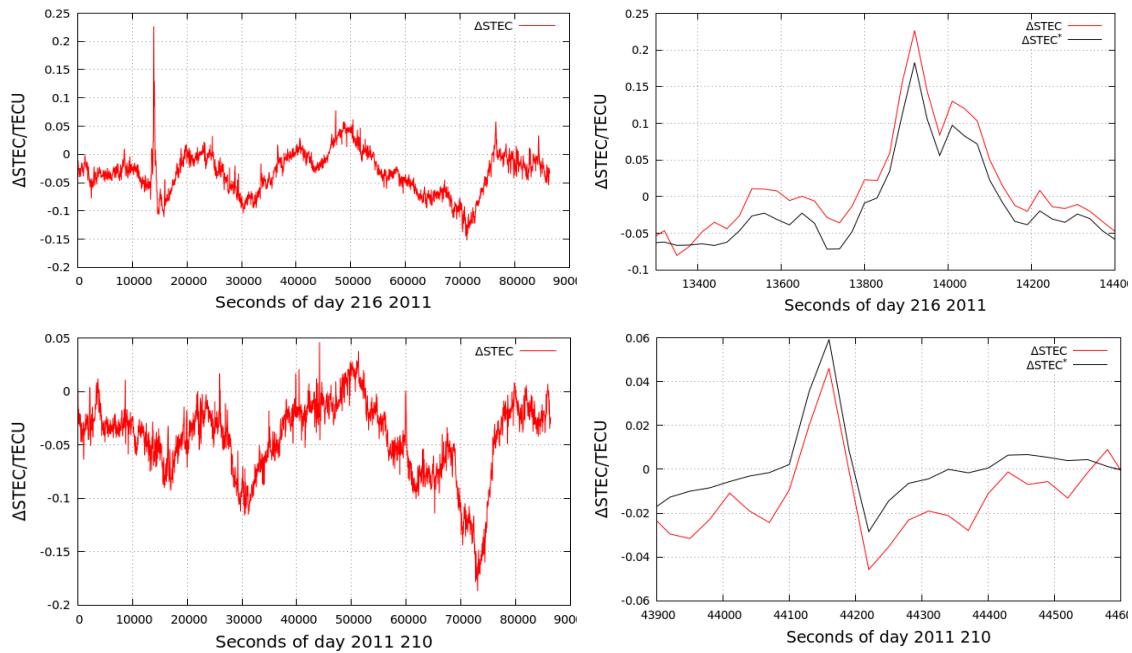
142

143 To sum up, there is no mistakes in our strategy and the disagreement regarding HP&GR is in how
144 the STEC variations corrected by the obliquity factor are named/interpreted. In this point, we
145 think that our interpretation is more adequate.

146

147 HP&GR also state that, due to these supposed mistakes, our results and conclusions could be
148 erroneous. After having processed data from an entire solar cycle, we have been able to
149 satisfactorily cross-check our results with those found in the literature: in our opinion, this task
150 is mandatory in any scientific work. For instance, Figure 2 depicts two of the examples that can
151 be found in Hernández-Pajares et al. (2012) and correspond to days 216 and 210 of 2011 (during
152 those days, two weak SF occurred, as reported in Hernández-Pajares et al. (2012)). Using the
153 same time intervals as in Hernández-Pajares et al. (2012), the panels on the right side show that
154 our $\Delta STEC$ detector is able to reproduce similar results to those in Hernández-Pajares et al.
155 (2012). Indeed, the amplitude of the peak reaches to 0.2 TECU. Additionally, the detection is
156 better if we use $\Delta STEC^*$ (a parameter also defined in our paper) because the noise is reduced
157 and the detection is clearer. However, this detection can be done only if short time intervals are
158 exclusively considered, as it has been done in the panels on the right side of Figure 1. In contrast,
159 if the time intervals are expanded to an entire day (as in the left panels), it can be observed that
160 in some instants, the values of $\Delta STEC$ can be at the same level as or even larger than the values
161 during the SFs. As shown in our paper, these results indicate the difficulty in establishing
162 thresholds for unsupervised SF detections using this detector.

163



164 **Figure 2.** Left column: $\Delta STEC$ at the SSP during two days of 2011: day 216 at the top and day
 165 210 at the bottom. Right column: in red, an enlarged view of the plots on the left side during the
 166 same time interval as in Hernández-Pajares et al. (2012). Additionally, $\Delta STEC^*$ is depicted in
 167 black.

168 3. Regarding the claim about the novelty of the SF detectors.

169 As mentioned in the introduction of the present answer, the goal of Curto et al., (2019),
 170 regarding the GNSS SF detectors, was not to present three new SF detectors but to analyse their
 171 suitability for the automatic detection of SF. In this sense, the key results pertaining to this goal
 172 are the three complementary distribution functions (CDFs) presented in the three panels in
 173 Figure 9 in Curto et al., (2019). Indeed, from Figure 9, our conclusion was that $\Delta STEC$ is not
 174 adequate for the automatic detection of SF. On the contrary, the two other detectors are more
 175 suitable for this automatic task.

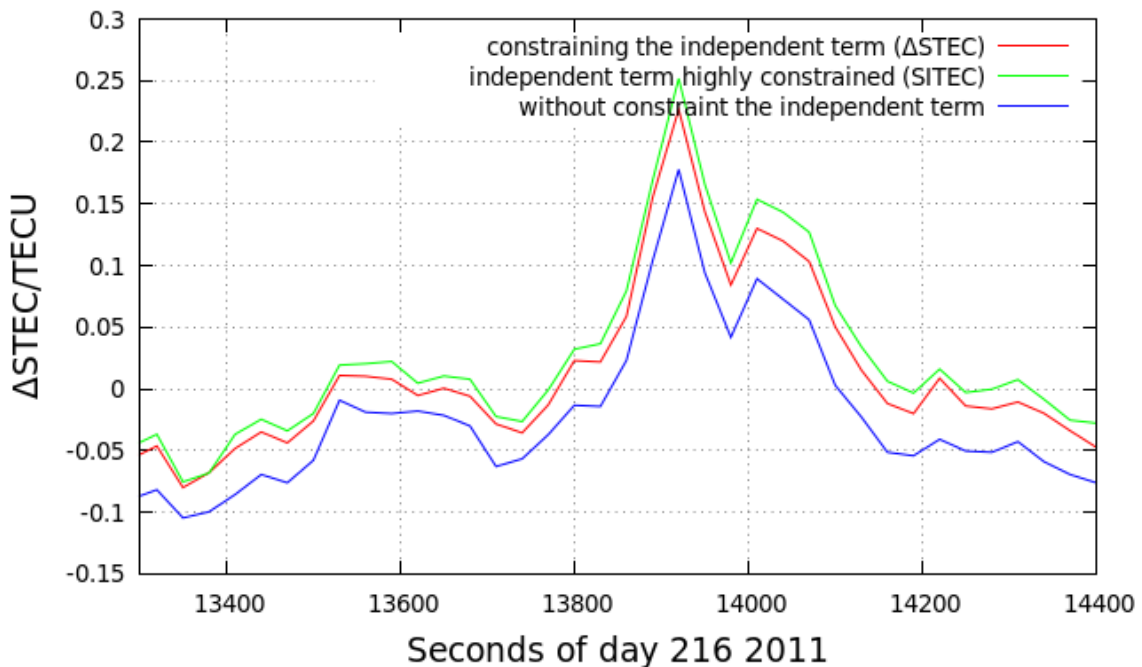
176
 177 We have not presented any of these SF detectors as a "new Solar Flare index", as HP&GR state
 178 in their comments. The only sentence that could be interpreted in this sense can be found at the
 179 end of section 2.2 *Data and Thresholding*:

180 *"In conclusion, the value of p can be used as a measure of the confidence level for SF detection.*
 181 *This is a novelty with respect to previous SF detectors based on GNSS measurements, because it*
 182 *represents a self-consistent way for providing confidence to the SF detections"*.

183 When we compared $\Delta STEC$ with the GNSS solar flare activity indicator (GSFLAI), we stated that
 184 they are "similar" (line 174) or "equivalent" (line 190) because, over the same events, the results
 185 obtained using our $\Delta STEC$ detector are very similar, but not exactly the same, to those
 186 presented in Hernández-Pajares et al. (2012) (see, for instance, the aforementioned Figure 2).
 187 There are several reasons that could explain these differences, some of which are the use of the
 188 slope (used in Hernández-Pajares et al. 2012) instead of $\Delta STEC$, the cadence of the data (1 s
 189 and 30 s) or the outlier exclusion strategies.

190 Moreover, note that the detector consists of more than just a model relating the angle between
 191 the IPP and solar zenith (χ) with each of $\Delta STEC_i^j$. For instance, Wan et al. (2005) proposed a

192 proportional relationship of the sudden increase in total electron content (SITEC) with $\cos \chi$ ¹,
 193 while Hernández-Pajares et al. (2012) defined *GSFLAI* by means of a linear relationship between
 194 $\Delta STEC_i^j$ and $\cos \chi$. The detector, i.e., the parameters of the relationship, also depends on how
 195 these parameters are estimated: Kalman filter or least squares, constraint/smooth equations,
 196 etc. In our case, a linear relationship was assumed (as *GSFLAI*) instead of a proportional one (as
 197 *SITEC*). However, we realized that dropping the independent term of this linear relationship, the
 198 results were still worse than those presented in the left panel of Figure 9 in our paper. Therefore,
 199 we decided to constrain the value of the independent term to zero in such a way that our
 200 detector, $\Delta STEC$, can be close to the *GSFLAI* or *SITEC* depending on the constraint imposed on
 201 the independent term. For instance, using the case presented in the top-right panel of Figure 1
 202 in this document, Figure 3 presents the $\Delta STEC$ using different constraints on the independent
 203 term: a moderate constraint, as it is used in $\Delta STEC$ (in red), a heavy constraint (in green), which
 204 should be equivalent to the *SITEC* in Wan et al. (2005), and no constraint on the independent
 205 term (in blue), which should be equivalent to the *GSFLAI* (assuming that the *GSFLAI* drops the
 206 independent term and considering the G2 definition for the *GSFLAI* that HP&GR mention in their
 207 document).
 208



209
 210 **Figure 3.** $\Delta STEC$ computed using three different constraints on the independent term of the
 211 linear fitting: without constraint (in blue), hard constraint (in green) and moderate constraint (in
 212 red).
 213

214 As shown, a moderate constraint on the independent term causes $\Delta STEC$ to behave within the
 215 *GSFLAI* and *SITEC* outputs. In this way, in this example, $\Delta STEC$ is closer to the *SITEC* than to the
 216 *GSFLAI*.
 217

218 In summary, there are some aspects of the implementation of the SF detectors that are not
 219 explicitly shown in the corresponding articles that describe the detector but that could affect
 220 their performance. This is the reason why we have compared only the results, concluding that
 221 they are similar, and for the same reason, we limited our conclusion to the poor performance of

¹ Actually, the relationship shown in the paper is the inverse of the Chapman function, but, as the authors state in their paper, it can be approximated as a relationship with $\cos \chi$.

222 $\Delta STEC$ as an automatic detector. However, in our opinion, this conclusion should be extended
223 to detectors based on the sudden increase in the STEC at the SSP (not only $\Delta STEC$ or the GSFLAI
224 but others defined in previous works, such as the case of the SITEC). Consequently, coming back
225 to the novelty, it would be a non-sense to present $\Delta STEC$ as a new automatic detector (as
226 HP&GR are claiming) and, after that, to conclude that it does not work as an automatic detector.
227 Therefore, this is an irrelevant discussion because, in our paper, we are not using $\Delta STEC$ or the
228 GSFLAI for automatic detections.

229

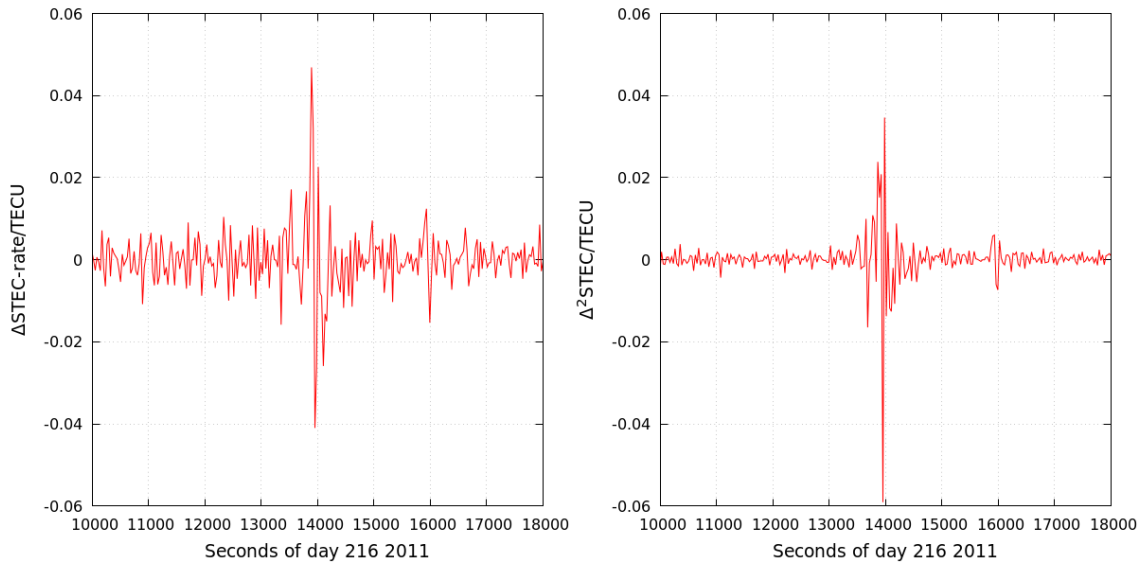
230 Finally, HP&GR state that, in previous works, they have used the second difference in time of
231 the VTEC at the SSP as an indicator of solar activity. Following the same line of thought as
232 HP&GR, one could state that the first difference in time of the VTEC at the SSP was used in
233 several works prior to Hernández-Pajares et al. (2012). Therefore, one should conclude that
234 there is no novelty in the GSFLAI definition. However, we think that this is not the case and that,
235 as we have commented before, in SF detection, it is important not only to determine which
236 physical property should be used to characterize the SF occurrence but also to select the
237 methodology necessary to obtain the corresponding parameters. Moreover, as we stated
238 before, in our work, we did not claim that the detectors were novel, but simply discussed the
239 best way to use them as automatic SF detectors, which, in the end, should be their goal.

240

241 For instance, HP&GR refer to Monte-Moreno and Hernández-Pajares (2014), where they used
242 the “*subsolar Vertical Total Electron Content double difference in time*” as an indicator of solar
243 activity. In fact, they used in this paper the difference in time (rate) of the GSFLAI (GSFLAIR)
244 which, in our case, should be similar to the rate of $\Delta STEC$. However, $\Delta^2 STEC$ is not equivalent
245 to the $\Delta STEC$ rate. Indeed, the first one is obtained by fitting a linear model to the satellite-
246 receiver $\Delta^2 STEC_i^j$, while the second one would be obtained by differencing in time $\Delta STEC$ at
247 the SSP. In this way, $\Delta^2 STEC$ should be the rate of $\Delta STEC^*$ defined in our paper. In order to see
248 the differences, Figure 4 depicts for the same example in Figure 3 the $\Delta STEC$ rate in the left
249 panel, and the $\Delta^2 STEC$ in the right panel. It can be seen that both detectors have similar peaks
250 when the SF occurs. However, the noise level of the $\Delta STEC$ rate is several times larger than the
251 noise in the $\Delta^2 STEC$ detector. Probably, this is the reason why Monte-Moreno and Hernández-
252 Pajares (2014) set a threshold of 0.025 TECU for the SF detection based on the “*experience of*
253 *the authors comparing with other sources*”. In our case, we set a threshold for $\Delta^2 STEC$ to just
254 0.01 TECU based in our statistic results, which are shown in the figure 9 of our paper (middle
255 panel). As it can be seen in this panel we are able to detect, in a confident way, much more SFs
256 than putting the threshold in 0.025 TECU.

257

258



259
 260 **Figure 4:** left panel, $\Delta STEC$ rate for the example depicted Figure 3. Right panel, $\Delta^2 STEC$ for the
 261 example depicted in Figure 3.

262 We have to recognize that we did not aware the work in Monte-Moreno and Hernández-Pajares
 263 (2014), otherwise we would remark in our work this improvement of $\Delta^2 STEC$ with respect to
 264 GSFLAIR.

265

266 4. References

267 Curto, J. J., Juan, J. M., & Timoté, C.C. (2019). Confirming geomagnetic Sfe by means of a solar
 268 flare detector based on GNSS. *J. Space Weather Space Clim.*, 9, A42.
 269 <https://doi.org/10.1051/swsc/2019040>

270 Hernández-Pajares, M., García-Rigo, A., Juan, J. M., Sanz, J., Monte, E., & Aragón-Àngel, A.
 271 (2012). GNSS measurement of EUV photons flux rate during strong and mid solar flares.
 272 *Space Weather*, 10(12). <https://doi.org/10.1029/2012SW000826>

273 Monte-Moreno E, Hernández-Pajares M (2014) Occurrence of solar flares viewed with GPS:
 274 Statistics and fractal nature. *Journal of Geophysical Research: Space Physics*,
 275 119(11):9216–9227. <https://doi.org/10.1002/2014JA020206>

276 Rovira-Garcia, A., Juan, J. M., Sanz, J., González-Casado, G., & Ibáñez, D. (2016). Accuracy of
 277 ionospheric models used in GNSS and SBAS: methodology and analysis. *Journal of Geodesy*,
 278 90(3), 229–240. <https://doi.org/10.1007/s00190-015-0868-3>

279 Rovira-Garcia, A., Ibáñez-Segura, D., Orús-Perez, R., Juan, J. M., Sanz, J., & González-Casado, G.
 280 (2019). Assessing the quality of ionospheric models through GNSS positioning error:
 281 methodology and results. *GPS Solutions*, 24(1), 4. <https://doi.org/10.1007/s10291-019-0918-z>

283 Wan W, Liu L, Yuan H, et al (2005) The GPS measured SITEC caused by the very intense solar
 284 flare on July 14, 2000. *Advance Space Research* 36:2465–2469.
 285 <https://doi.org/10.1016/j.asr.2004.01.027>